Extended data for

Visual pathway origins: connectome of a human foveal retina

Yeon Jin Kim[1], Orin Packer[1], Thomas Macrina[2], Andreas Pollreisz[3], Christine A. Curcio[4], Kisuk Lee[2], Nico Kemnitz[2], Dodam Ih[2], Tri Nguyen[2], Ran Lu[2], Sergiy Popovych[2], Akhilesh Halageri[2], J. Alexander Bae[2], Joseph J. Strout[2], Stephan Gerhard[5], Robert G. Smith[6], Paul R. Martin[7], Ulrike Grünert[7], Dennis M. Dacey[1,8,*]

[1]Department of Neurobiology & Biophysics, University of Washington, Seattle, WA, 98195

[2]Zetta AI LLC, Sherrill, NY, USA

[3]Department of Ophthalmology, Medical University of Vienna, Vienna, Austria

[4]Department of Ophthalmology and Vision Sciences, University of Alabama at Birmingham, Alabama 35294

[5]Aware LLC, Rappenstrasse 19, 8307 Effretikon, Switzerland

[6]Department of Neuroscience, University of Pennsylvania, Philadelphia, PA 19104

[7]The University of Sydney, Save Sight Institute and Discipline of Ophthalmology, Faculty of Medicine and Health, Sydney, NSW, 2000, Australia

[8]Washington National Primate Research Center, Seattle, WA 98195

*Corresponding author: Dennis M. Dacey (dmd@uw.edu)

This PDF file includes:

Extended Data Figures 1 to 10

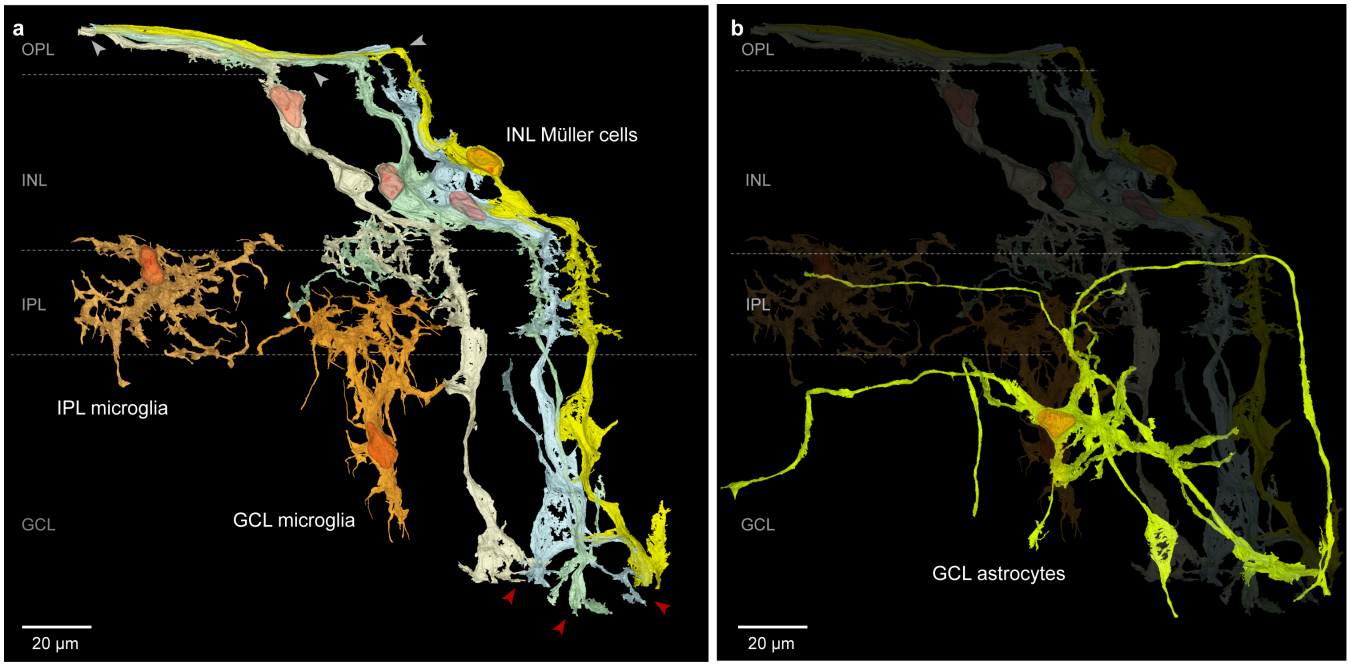

Extended Data Fig. 1. Non-neuronal cells. a. Non-neuronal cells were divided into 3 types. Müller cells with cell bodies in the INL (INL Müller) were vertically oriented, extending outward processes into the Henle fiber layer ensheathing cone axons (white arrowheads) and inward processes to the inner surface of the retina (red arrowheads, Müller endfeet). A very small population of microglia (15 cells) was present in the IPL with cell bodies near the INL-IPL border (IPL microglia; 10 cells) or in the GCL with processes that extended into the IPL (GCL microglia, 5 cells) and that showed a characteristic dendritic morphology and ultrastructure that distinguished them from Müller cells (see also Extended Data Fig. 3a-3c). **b.** A third population of glial cells was present in the GCL (26 cells, GCL astrocytes). Cell bodies of these cells were often apposed to blood vessels and the long curving processes also tended to appose blood vessels resulting in an overall stellate and tortuous branching pattern. The location of these cells in the GCL and their close relationship with the inner retinal vasculature suggests strongly that they correspond to astrocytes.

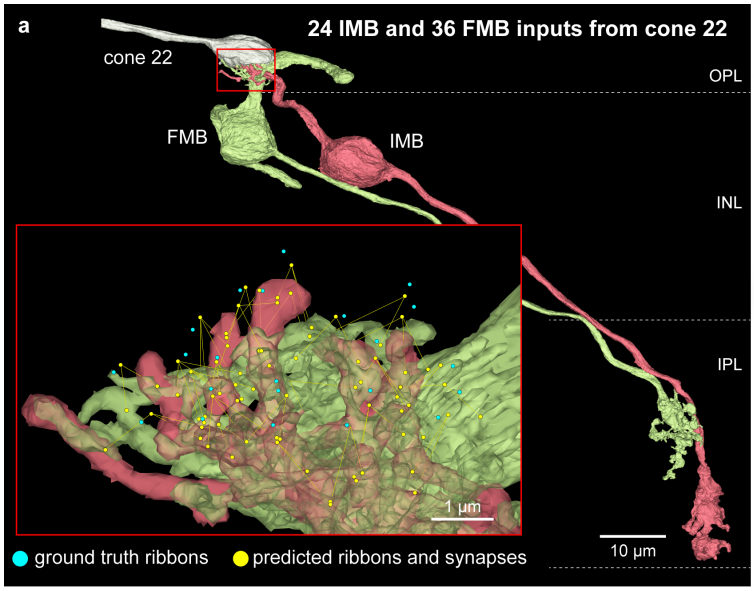

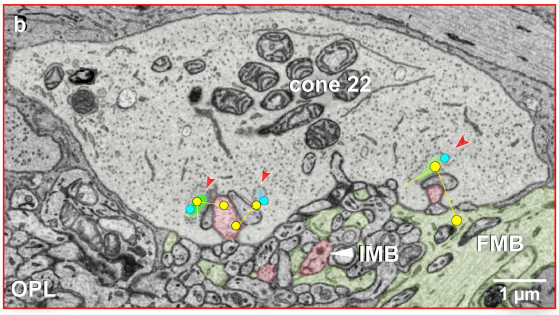

c

LM	ribbon precision	ribbon sensitivity	ribbon total (#)	synapse precision	synapse sensitivity	synapse total (#)
cone 21	100 %	100 %	12	98 %	100 %	43
cone 22	88 %	100 %	22	98 %	99 %	61
cone 58	89 %	100 %	17	100 %	100 %	49
Average	92.3 %	100 %	17	98.7 %	99.7 %	51
SD	6.7 %	0 %	5	1.2 %	0.6 %	9

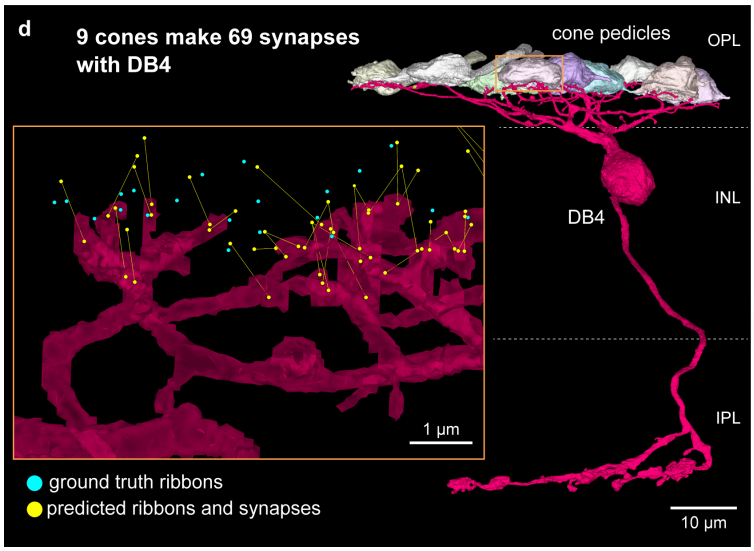

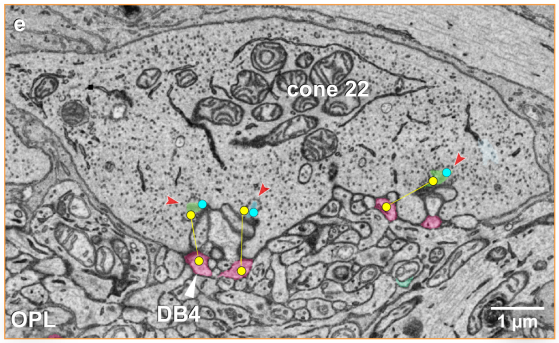

f

Bipolars	synapse precision	synapse sensitivity	synapse total (#)
DB4	87 %	95 %	73
DB2	89 %	89 %	53
Average	88.0 %	92.0 %	63
SD	1.4 %	4.2 %	14

Extended Data Fig. 2. Further evaluation of excitatory and conventional synaptic detection. a. Ribbon identification and synaptic prediction between cone 22 and FMB and IMB. 3D view shows cone 22 pedicle (white) and inner-ON (IMB, light orange) and outer-OFF (FMB, light green) bipolar cells. Cone 22 made 24 and 36 contacts with the IMB and FMB cell respectively (one false positive ribbon was predicted for Cone 22). Inset shows the dendritic terminals of the two bipolar cells. Ground truth identification of cone ribbons (blue dots) and predicted ribbons and synaptic connections (yellow dots and lines) are shown. **b**. Single EM layer view through cone 22 shows ribbon segmentation (ribbons in varied colors) and two predicted synaptic connections (yellow dots and lines) made with both IMB and FMB dendrites. **c**. Table shows precision and sensitivity for all midget bipolar connections made by cones 21, 22, and 58. **d**. As in **a**, but for a single diffuse bipolar cell (classified as a DB4 type) that also was postsynaptic to cone 22 and eight additional cones. This DB4 cell made 69 contacts (both basal

and invaginating contacts) with the nine cone pedicles. Inset convention as in **a** showing synaptic predictions for the connection with cone 22. **e**. Conventions as in **b**, showing three predicted basal contacts between cone 22 and this DB4 cell. **f.** Table on left shows precision and sensitivity of synaptic predictions for the DB4 cell and a DB2 cell that was postsynaptic to eight cones, including cone 22.

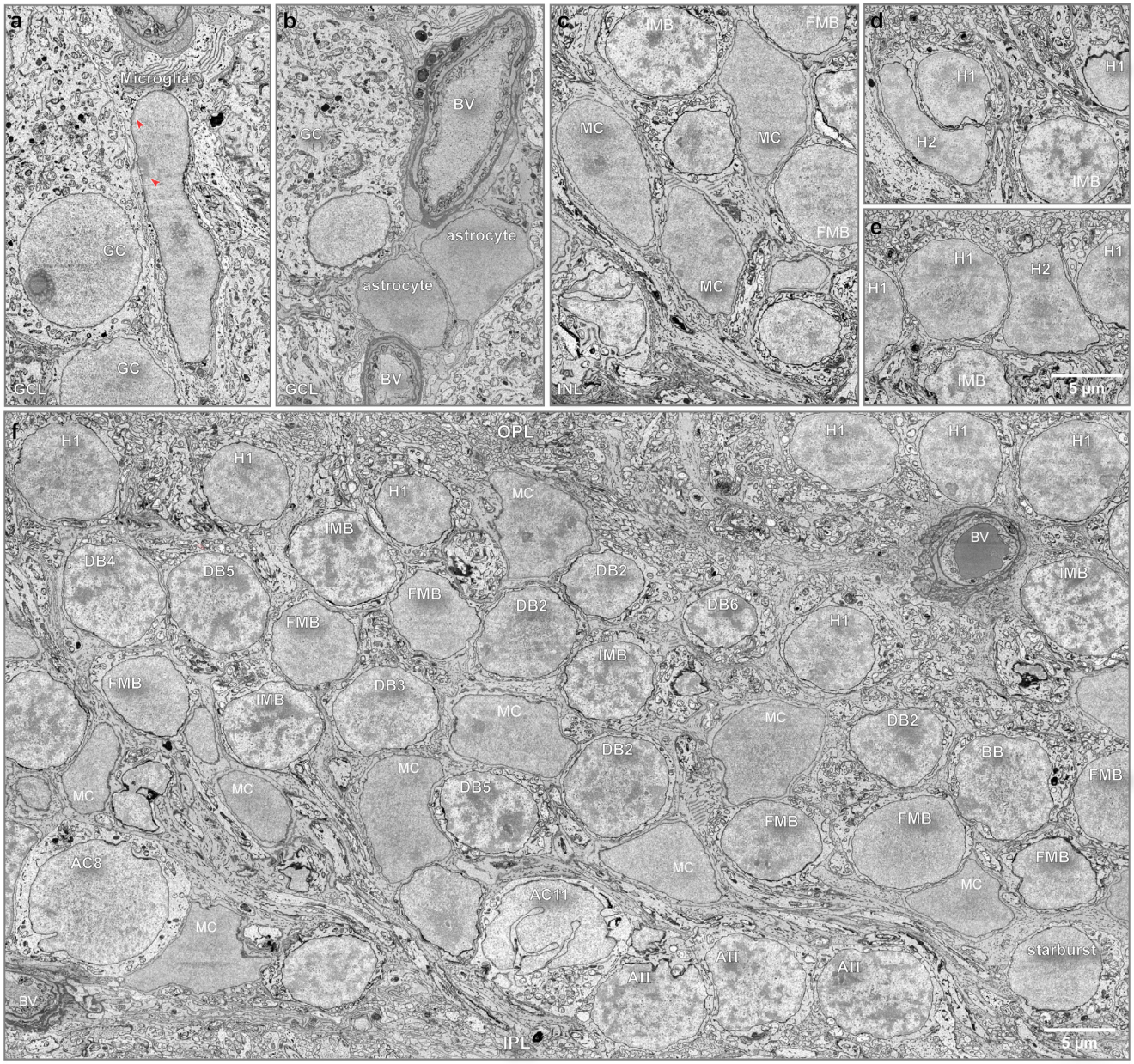

57

58 **Extended Data Fig. 3. Distinguishing cell types by morphology of the nucleus.** Examples from
59 single layer EM view of nuclear morphology in identified (segmented) cell types in the inner nuclear and
60 ganglion cell layers (INL, GCL). **a.** Microglia cells were easily recognized by their distinctly elongated
61 nucleus, with heterochromatin accumulated at the nuclear margins (red arrowheads). All ganglion cells
62 (GC) have round, euchromatic nuclei. **b.** Astrocytes were present in the GCL, and their cell bodies
63 tended to accumulate around blood vessels; nuclei were relatively darkly stained and euchromatic. **c.**
64 Müller glia cells (MC) were recognized by very large, ovoid or irregularly-shaped nuclei. Müller cell
65 nuclei were euchromatic and moderately stained and similar in appearance to astrocyte nuclei but

appeared larger. By contrast, the nuclei of bipolar cells (BC) are rounded. Invaginating-ON (IMB) midget bipolar cells show distinct heterochromatic nuclear staining marked by alternating very darkly and lightly stained regions. By contrast flat midget bipolar cells (FMB) show light euchromatic staining. **d and e**. H1 and H2 horizontal cells both show heterochromatic nuclear staining, but the dark-light contrast is less than that shown for the IMB cells. H1 cells have rounded nuclei, whereas the nuclei of H2 cell nuclei are irregularly shaped. **f.** Overview of nuclear patterning in the inner nuclear layer (INL). Like IMB cells, other inner stratifying-ON bipolar types (DB4, DB5, DB6 and BB) all show darkly stained, dense heterochromatic nuclear staining. However, unlike FMB cells the other outer stratifying OFF-bipolar cells (DB1, DB2, DB3) show lighter stained heterochromatic nuclei (a DB1 nucleus does not appear in this image), similar to H1 horizontal cells. Along the inner border of the INL amacrine cells display diverse nuclear morphologies. Starburst amacrine cells (see Fig. 4c) show round, lightly stained euchromatic nuclei; the starburst shown is an OFF-starburst with soma in the INL; ON-starbursts in the GCL (see Extended Data Fig. 3f) show the same nuclear morphology as OFF-starburst cells. AII amacrine cells (Fig. 4a) are located at the border with the inner plexiform layer (IPL*)*. They show some scalloping of the nuclear envelope and are strongly heterochromatic, similar in appearance to ON bipolar cells. Other amacrine cell types are further distinguished by the degree of infolding of the nuclear envelope (crenulation) together with the distribution of chromatin. The small field A11 amacrine cells (see Fig. 4e) show extremely infolded nuclear envelopes and light heterochromatic staining. By contrast with the AC11 cell, the large field AC8 amacrine cell shows less crenulation and euchromatic nuclear staining. See Figures S6 and S8 for additional examples of distinctive nuclear morphology in amacrine cell types. BV, blood vessels.

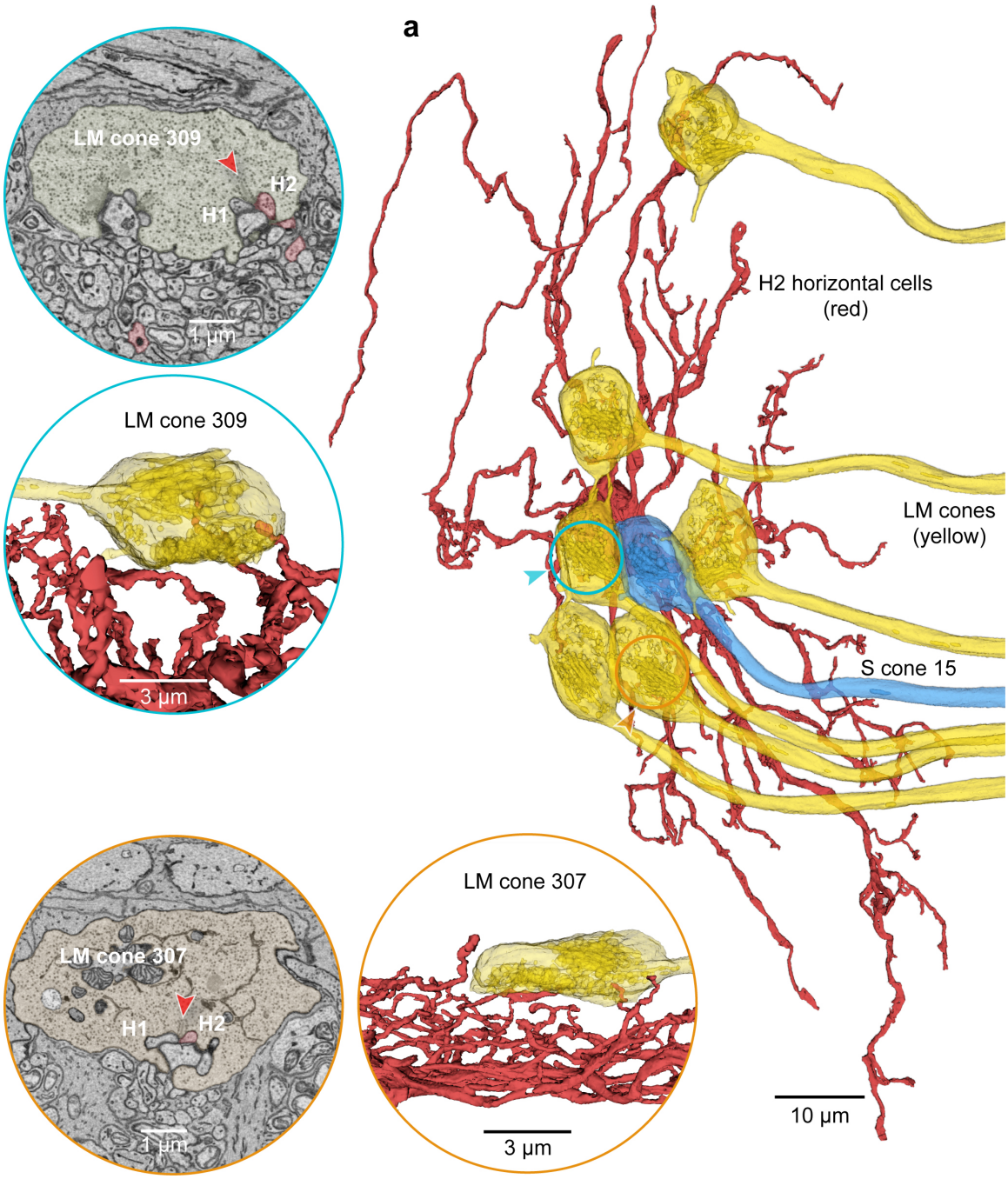

87

88 **Extended Data Fig. 4. H2 horizontal cells only sparsely contact LM cones. a.** In HFseg1 H2 cells
89 are sparsely branching and show little overlap with neighboring cells of the same type. A single H2 cell
90 (red) is shown in relation to 6 LM cone pedicles (yellow) and 1 S cone (blue, S cone 15; see main Fig. 2
91 for S cone connectivity). The cone pedicles are shown in partial transparency. The blue circled LM cone
92 (LM cone 309, blue arrowhead) is shown in the insets at the upper left. This cone is contacted by only 1
93 lateral element from this H2 cell; top inset shows a single layer EM view, and the lower inset shows a

3D view. By contrast H1 cells made 51 contacts with this cone accounting for 98.1% of the lateral elements. A second orange circled cone (LM cone 307, orange arrowhead) showed a similar pattern of horizontal cell connectivity, again making a single lateral contact with this H2 cell (1.8% of lateral elements), and 55 contacts with H1 cells (98.2% of lateral elements). This connection pattern was proofread for accuracy. Together with main Figure 2 the data analyzed thus far shows that H1 cells receive major input from all three cone types.

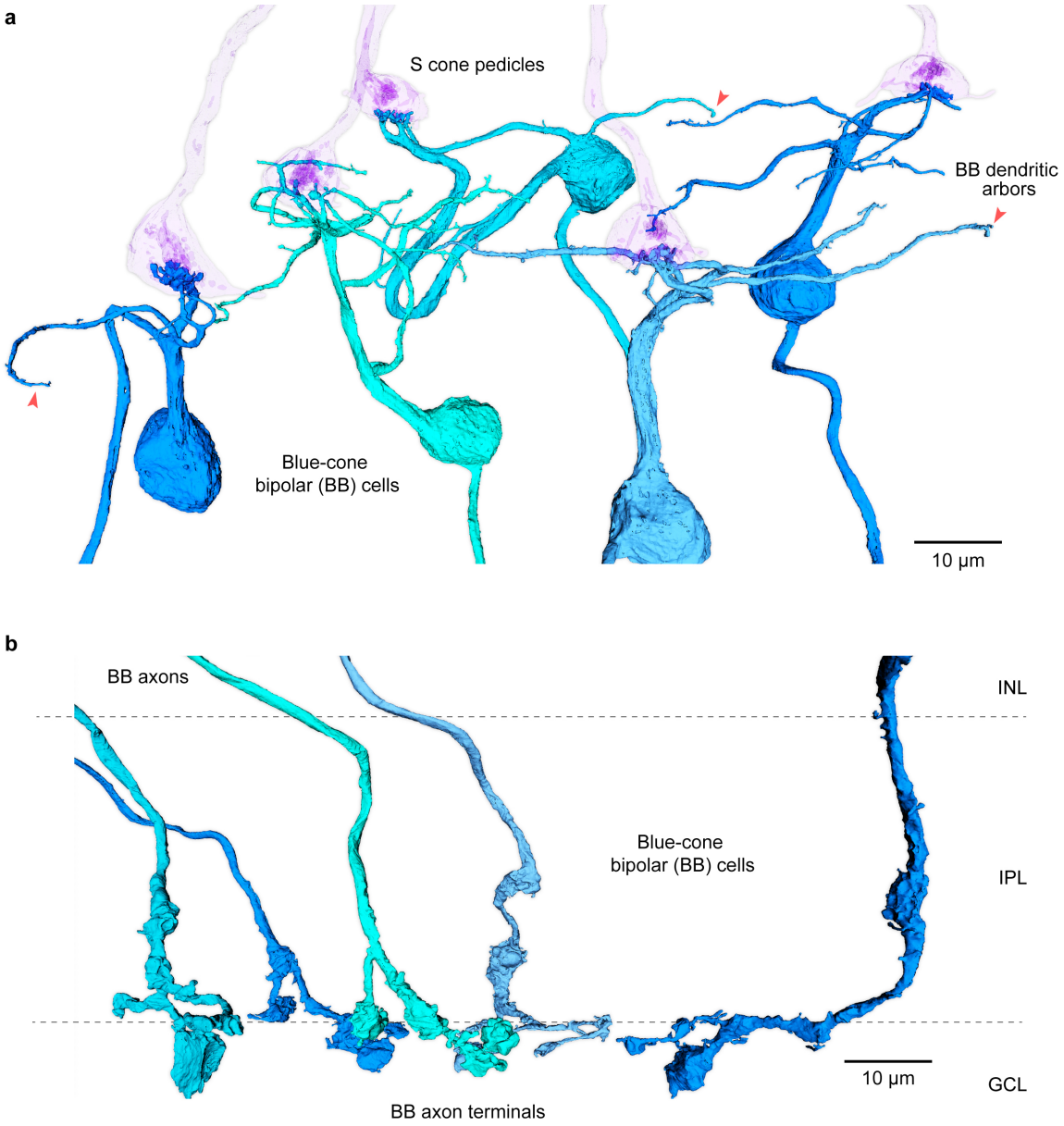

Extended Data Fig. 5. Blue cone bipolar cells (BB cells) show a distinctive dendritic morphology and axonal stratification. a. Dendrites of BB cells primarily target S cone pedicles where they make invaginating contacts. Five S cones are shown in partial transparency (violet), tilted slightly off the horizontal plane. These S cones are contacted by the dendrites of five BB cells (in shades of blue); there is a tendency at this foveal location for each S cone to be presynaptic primarily to a single BB cell. Primary dendrites of the five BB cells are indicated by red arrowheads. **b.** The axon terminals of these five BB cells are shown in a vertical view (image is also rotated relative to the view in **a**). The axons terminate along the inner border of the IPL often extending terminal varicosities across the outer border of the ganglion cell layer (GCL).

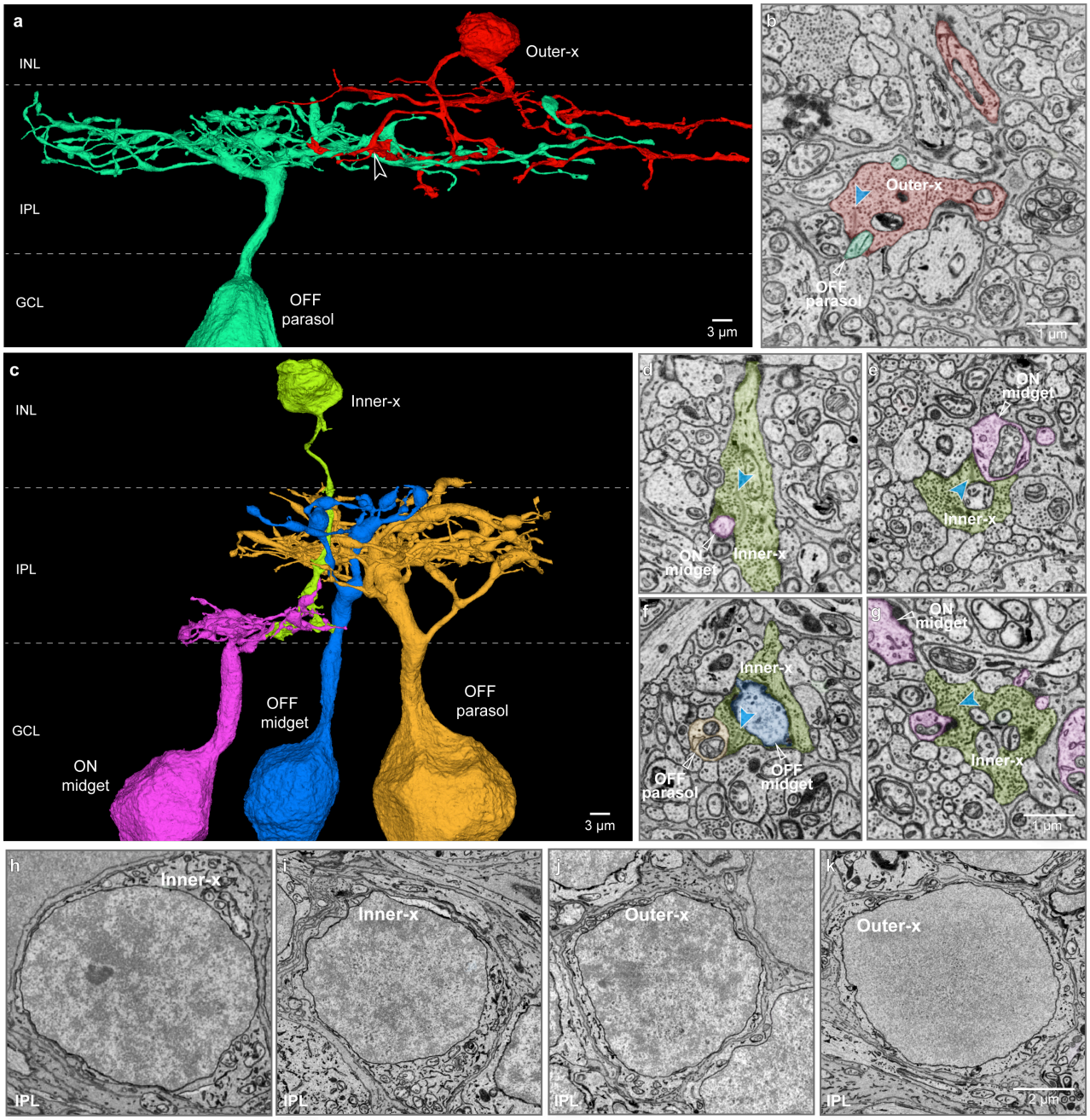

Extended Data Fig. 6. Inner- and Outer-x cells show amacrine like morphology, but, like bipolar cells make ribbon synapses in the IPL with ganglion cells. The x cells vary in morphology and depth of stratification in the IPL and do not form any consistent spatial mosaic patterns typical of either bipolar or amacrine cells. **a.** An Outer-x cell with sparse broadly stratifying branches in the outer half of the IPL. It is presynaptic to an OFF-parasol GC (teal) (as well as other amacrine and ganglion cell processes, including OFF midget GCs (not shown)). **b**. Ribbon synapse (blue arrowhead) from the OFF-x cell shown in **a** to an OFF-parasol cell dendrite (indicated by open white arrowhead in **a**). **c**.

Inner-x cell with a small axonal arbor stratified in the inner half of the IPL. **d-g**. Examples of ribbon synapses (blue arrowheads) made by the Inner-x cell shown in **c** with OFF parasol, OFF midget and ON midget GCs. Synaptic ribbons are indicated by blue arrowheads. **h-i**. Inner-x cells show light heterochromatic nuclear staining. **j-k**. Outer x-cells show both heterochromatic staining (**j**), like that of outer DB cells, and light euchromatic staining (**k**) like that of FMB cells suggesting that the x cells may reflect modifications in the morphology of some number of bipolar types including IMB, FMB and DB cells.

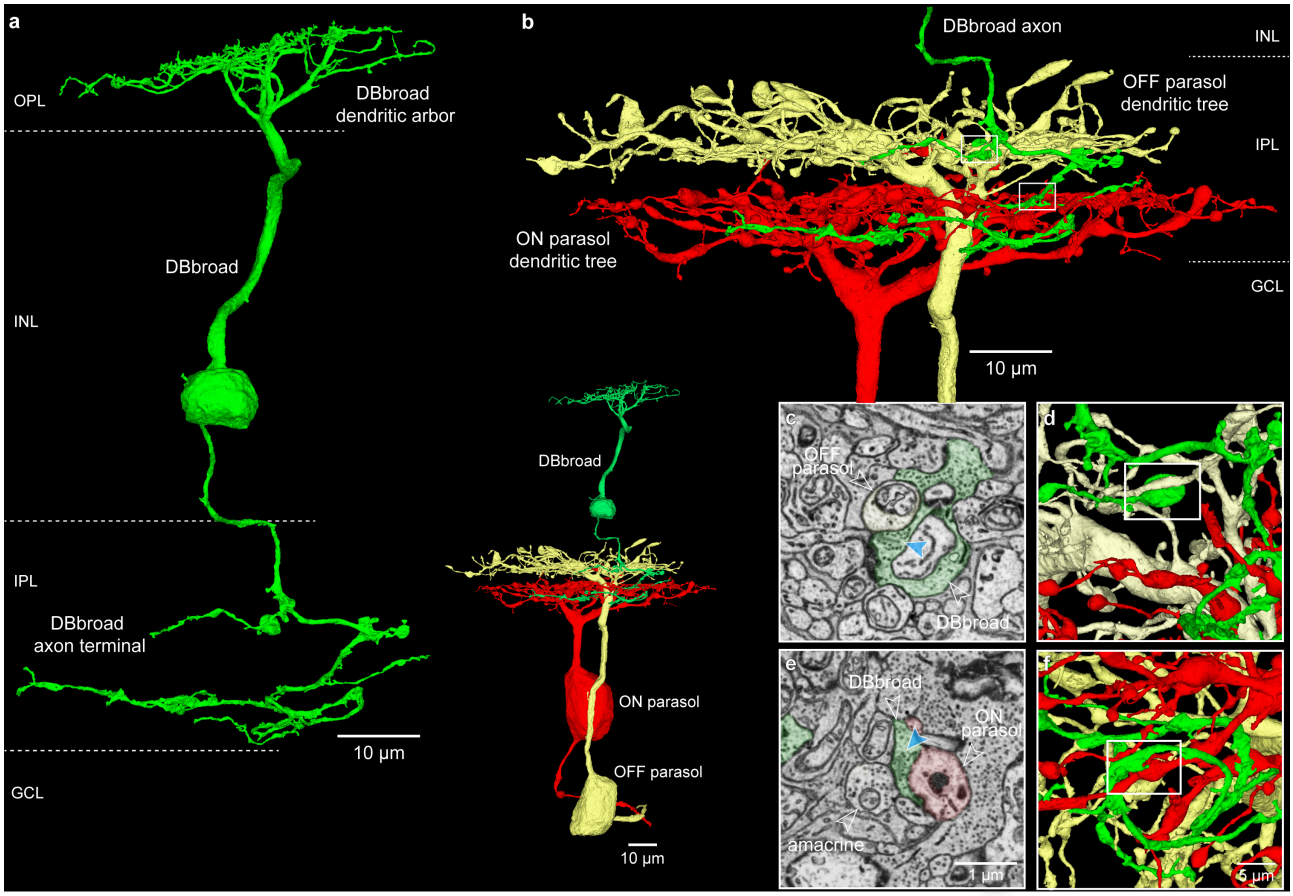

Extended Data Fig. 7. Distinctive morphology of DBbroad cells. DBbroad cells do not appear to correspond to any previously identified cone bipolar cell type in primate retina. These cells have broadly stratifying axons and make sparse ribbon synapses in both the outer (OFF) and inner (ON) portions of the inner plexiform layer. **a.** The axonal arbor of the DBbroad cell is large and sparsely branching and does not show distinctive or large synaptic varicosities. **b**. This DBbroad cell is presynaptic to both an outer-OFF and an inner-ON parasol ganglion cell; a vertical view of the three cells is shown in the inset at center. At the upper right is a zoomed view of the axonal arbor of the DBbroad cell and the dendritic trees of the two parasol cells (ON cell, red; OFF cell, yellow). **c-d**. Ribbon synapse (blue arrowhead) made with the OFF parasol cell (yellow, open arrowhead) shown in a single section view. Location of this synapse in 3D view is outlined by the white box in **d**. **e-f**. Synapse made with the ON parasol cell (red, open arrowhead), and an amacrine cell (open arrowhead) in **e** shown in a single section view. Location of this synapse in 3D view is outlined by the white box in **f**. Approximate synaptic locations shown in **d** and **f** are also indicated by the white boxes in **b**.

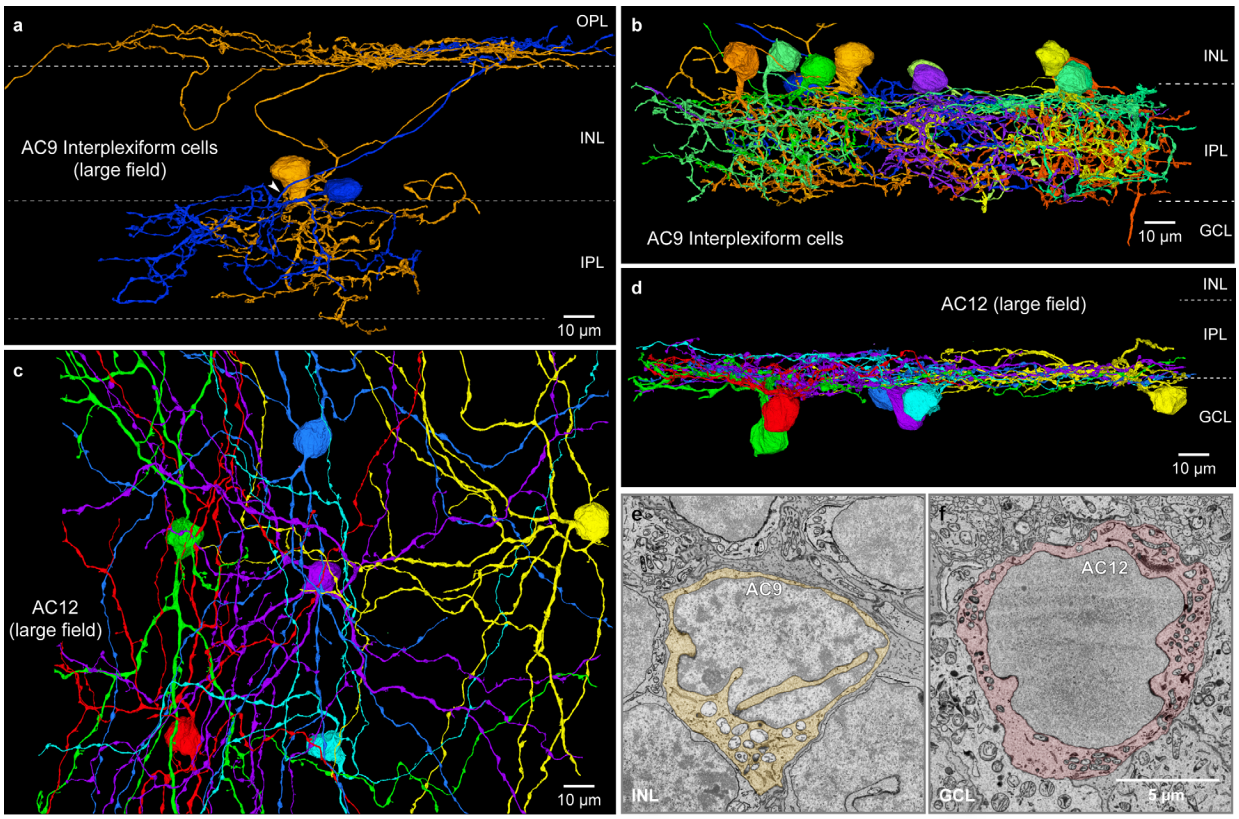

142

143 **Extended Data Fig. 8. Additional amacrine cell populations in the fovea. a.** AC9 is a large field
144 amacrine type that shows the distinctive morphology of interplexiform cells (cells with processes in both
145 outer and inner plexiform layers). A single axon-like (white arrowhead) process extends vertically from a
146 primary dendrite in the IPL into the OPL where it branches and extends laterally; the inner processes of
147 the cells are large, sparsely branching and tortuous extending across the full depth of the IPL. The
148 synaptic connections of the outer and inner processes remain to be investigated. **b**. Vertical view of the
149 dendritic trees of ten AC9 cells in the IPL (complete demonstration of all axon-like processes and their
150 synaptic connections will require additional proofreading of each cell). **c.** AC12 is large field amacrine
151 type with cell bodies displaced to the ganglion cell layer (GCL). Shown here a horizontal view of six A12
152 cells, the dendrites are thick, radiate and moderately branched, similar in appearance to the AC8 cells
153 shown in Fig. 4g. **d.** Vertical view of the same mosaic of AC12 cells; these cells stratify broadly over the
154 inner third of the IPL where they costratify with and synapse onto the axon terminals of midget bipolar
155 (IMB) cells (not shown). Details of the synaptic relationships of this cell type and its relationship to
156 amacrine types previously identified in human and non-human primate retina remain to be clarified.
157 AC9 and AC12, like other amacrine types show distinctive nuclear shapes and staining patterns. **e**. AC9
158 shows a highly infolded nuclear envelope combined with dark heterochromatic nuclear staining. **f**. AC12
159 shows scalloped-irregular nuclear envelope combined with light euchromatic nuclear staining.

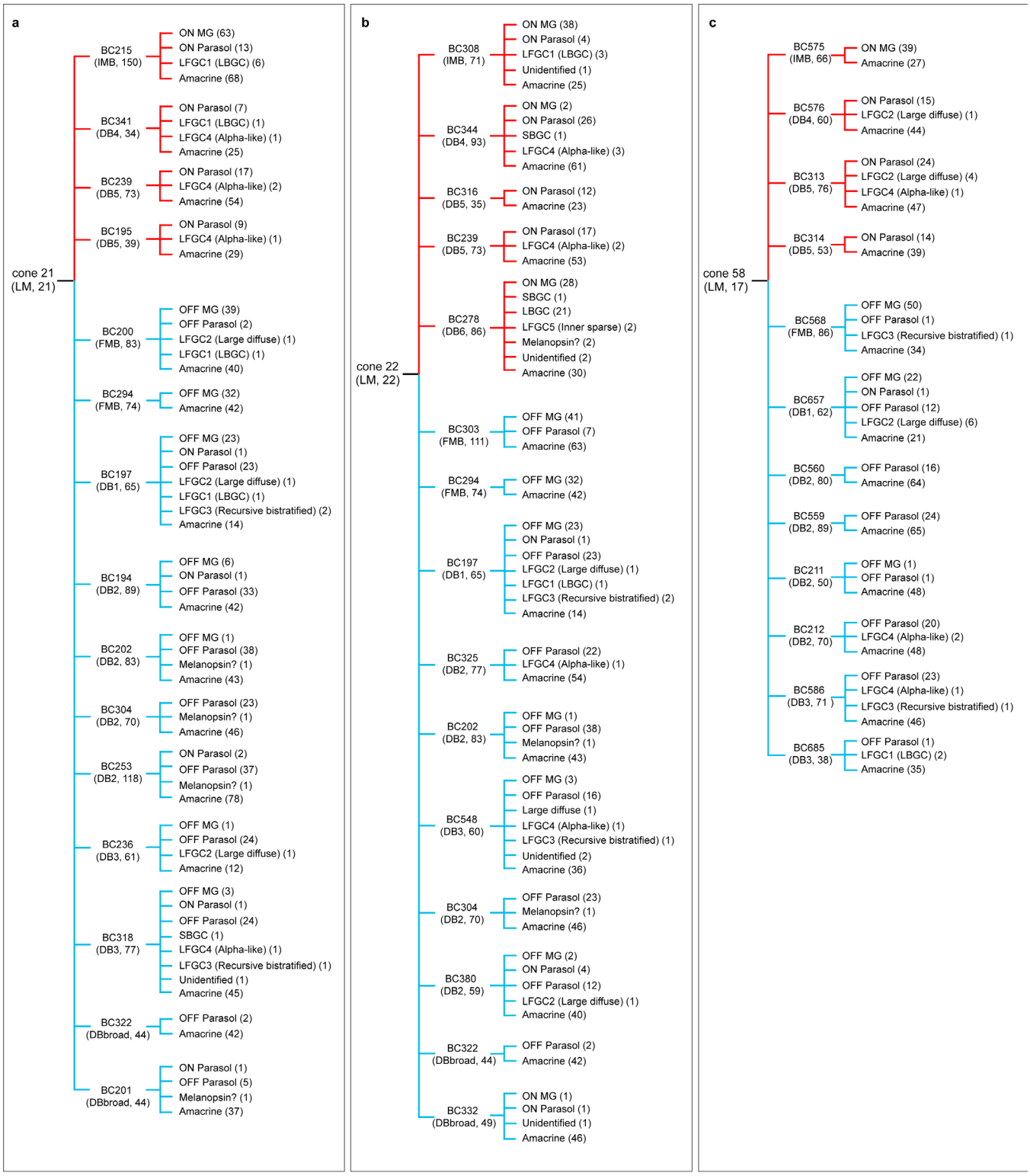

Note: as examples, cone 21 (LM, 21) indicates (cone type, # of total ribbon), BC215 (IMB, 150) indicates (bipolar type, # of total synapse).

Extended Data Fig. 9. Vertical excitatory connectome: outgoing synaptic contacts from all bipolar cells connected to 3 LM cones. The bipolar type and number of synapses is shown in

parentheses (e.g., BC 215 (IMB (cell type), 150 (outgoing synapses)). Synapses directed to ganglion cells were identified by type. Synapses directed to amacrine cells were summed and not yet divided by amacrine type). It can be noted that the total number of cells and synapses arising from OFF-bipolar types (blue connecting lines) is much higher than that for ON-bipolar cells (red-connecting lines); moreover, OFF bipolar cells are presynaptic to both ON and OFF ganglion cells whereas ON bipolar cells connect exclusively to inner ON ganglion cell types. It can also be noted that midget and parasol ganglion cells share significant convergent input from multiple bipolar cell types. These factors account for the high number of synapses in OFF visual pathways compared to ON pathways, as shown in Fig. 8c.

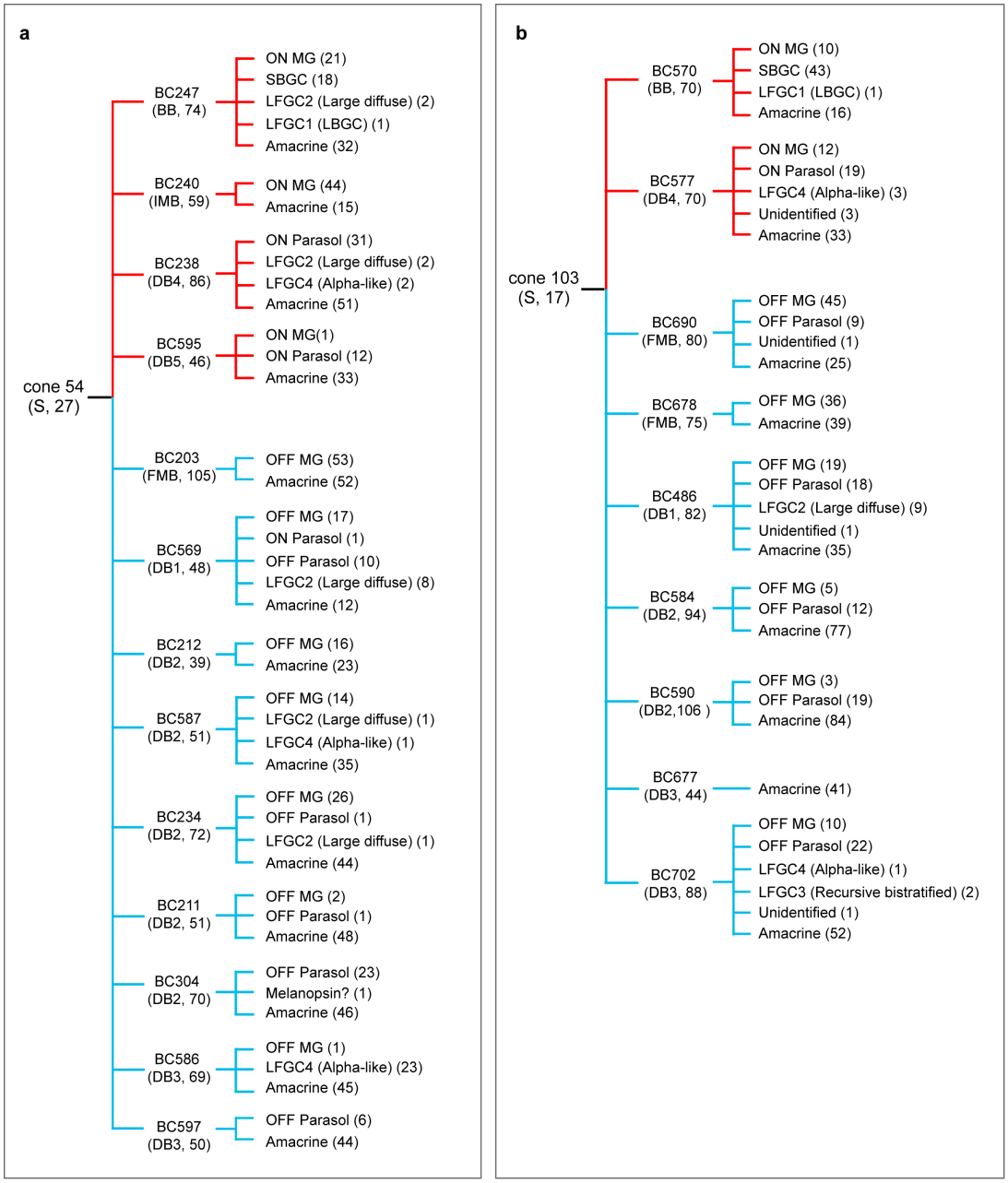

Note: as examples, cone 54 (S, 27) indicates (cone type, # of total ribbon), BC247 (BB, 74) indicates (bipolar type, # of total synapse).

Extended Data Fig. 10. Vertical excitatory connectome: outgoing synaptic contacts from all bipolar cells connected to the 2 S cones. The bipolar type and number of synapses is shown in parentheses (e.g., BC 247 (BB (cell type), 74 (outgoing synapses)).